

Improvement of voltage source inverter for photovoltaic energy conversion system dedicated to pumping applications

Abdelouahed Mesbahi, Ayoub Nouaiti, Abdallah Saad, Mohammed Khafallah

Laboratoire Energie et Systèmes Electriques Hassan II University ENSEM Casablanca Morocco

Abstract: This work presents a study and implementation of two topologies of a DC-AC inverter used in photovoltaic energy conversion chain applications. The proposed inverters are based on a full bridge associated to two level boost chopper to generate three or five levels. The proposed inverter has the benefit of using fewer components, less number of switches, high efficiency and delivering fewer harmonics. The deployment of techniques using a Selective Harmonic Elimination Pulse Width Modulation aims to reduce filter congestion and also improve the efficiency of the pumping system. Simulation results were verified on PSIM and validated on real experimental setup. The commands are implemented on a midrange microcontroller to drive controlling single phase motor associated to a water pump.

Keywords: photovoltaic energy conversion System, multilevel boost converter, multilevel inverter, Selective Harmonic Elimination, single phase induction motor

1. Introduction

For everyday life, access to clean water is essential in all deserted regions. So, people pain to extract water for their own needs, their own livestock, irrigation of land and many other uses.

Photovoltaic energy becomes today a promising energy. The use of this type of energy is suitable for rural countries where the power is not always available and the connection to grid is more expensive.

Different pumps are available for water pumping, among those centrifugal pumps are mostly used. The output voltage of PV Array is DC which can drive directly a Permanent Magnet Direct Current (PMDC) coupled to the pump shaft. Actually, almost the water pumps are driven by Single Phase Induction Motor (SPIM). The SPIM motor is preferred to the three phase version principally for its cost.

In the photovoltaic energy conversion System (PECS), the DC power produced by the PV panel is provided to load via different stage especially in the conversion of direct current (DC) to alternating current (AC) [1].

In solar inverters, the power switches have to support high voltage stresses. These inverters also have the problem of introducing large harmonic contents in the output voltage which increase the machine losses and affect their performances. Perfect commands and the multilevel topologies, can overcome these problems. They have advantages like low harmonic distortion, improved power quality, reduced voltage stress across the switches, less electromagnetic interference and reduction in the filter size. [2]-[5].

The topologies of multilevel inverters can be summarized in three categories [6] diode-clamped [7], flying capacitor or multicell [8]-[9], cascaded H-bridge [10]. Some variety of topologies are derived from these and simplified H-bridge multilevel [11].

The goal of the multilevel inverters is to obtain a clean voltage output with a Total Harmonic Distortion (THD). This is done with a considerable number of switches added to other components causing at the same time unbalancing voltage across capacitors. Researchers aim to ameliorate control techniques by decreasing the number of switches and reducing manufacturing price.

2. Description

The platform of the PECS is depicted in Figure. 1. It is composed by two Photovoltaic panels, a boost chopper and a full bridge single phase DC-AC inverter to supply water pump.

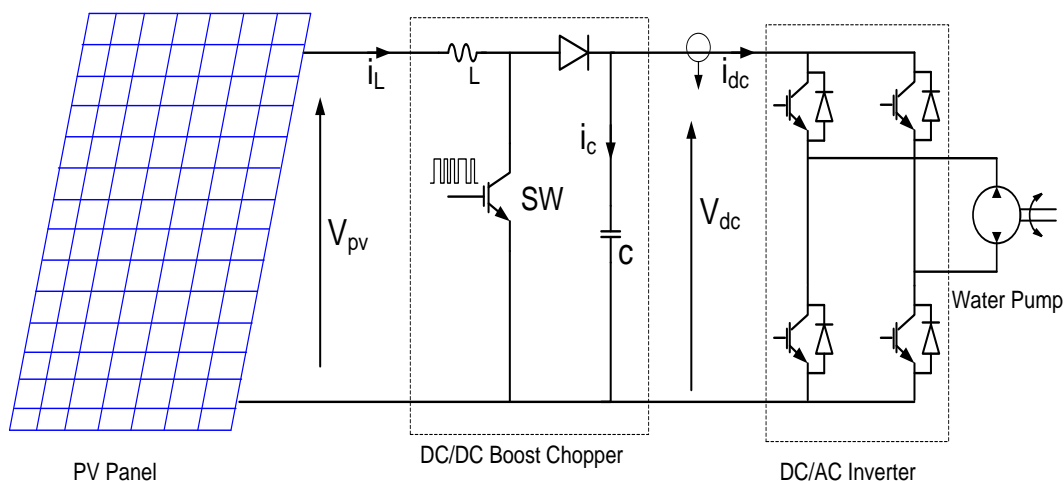


Figure.1. PECS platform

2.2 Photovoltaic panel model

The Sillicium p-n junction cell is the main part for designing a PV panel. This PV cell converts sunlight energy directly into electrical energy. The equivalent circuit of PV cell is done in Figure.2

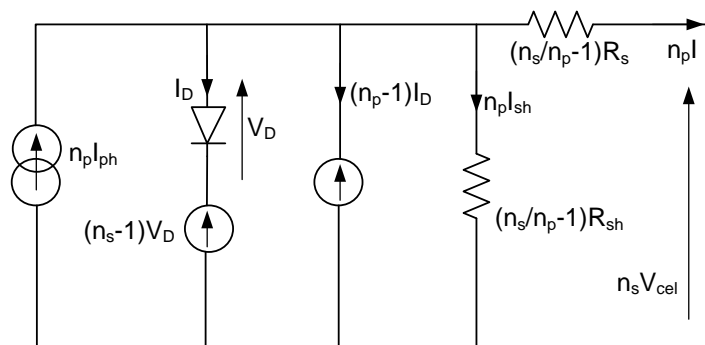


Figure.2. PV Panel equivalent circuit

To achieve a rated power, a number of PV cells are connected in series parallel forming PV modules and PV arrays. The PV modules or arrays can be modeled as a current source as in (1) [2]. the power output of a PV panel is given by adding the power of each cell depending on conditions of ambient temperature and solar irradiance

$$I = n_p I_g - n_p I_{rs} \left[\exp \left(\frac{q}{kTA n_s} V \right) - 1 \right] \quad (1)$$

2.2 Boost Chopper

The role of the DC Boost Chopper (BC) is to control the PV panel power output and is illustrated in Figure.1. It's composed by a power IGBT or MOSFET switch (SW) with an inductor and a capacitor. By switching ON the SW, the energy is first stored in inductor and then transferred to the VSI via the capacitor when SW goes OFF [12]

The BC output voltage is expressed in (2)

$$V_{dc} = \frac{T}{T - T_{ON}} V_{pv} = \frac{V_{pv}}{1 - D} \quad (2)$$

With $D = \frac{T_{ON}}{T}$ is the duty cycle.

Different structures of multilevel boost converter (MBC) have been developed. The three major topologies are:

- diode clamped, also called neutral point,
- capacitor clamped, also called flying capacitor,
- Cascaded multi-cell.

From those ones, the topology retained for this work is presented in Figure.3 [13].

The MBC output voltage is expressed in (3)

$$V_{OUT} = n \cdot V_{dc} = n \cdot \frac{V_{pv}}{1 - D} \quad (3)$$

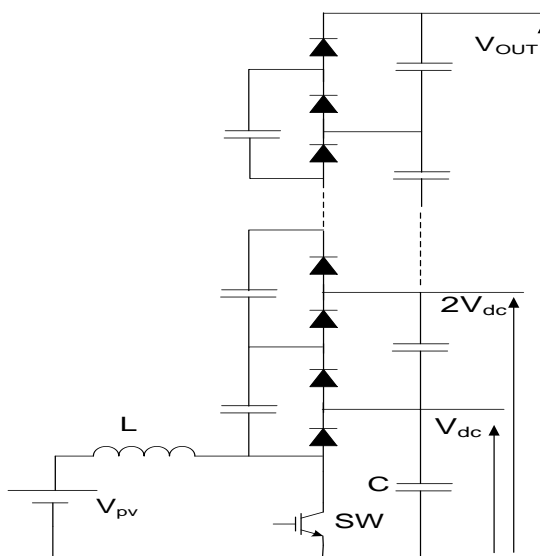


Figure.3. Multilevel boost chopper topology

2.3 Voltage Source Inverter

The DC output voltage of the boost converter has to be converted in AC form by a DC-AC single phase inverter bridge for providing electric power to water pump. Sinusoidal Pulse Width Modulation Technique (SPWM) is used to generate gating signals for PWM Inverter devices by comparing a triangular carrier wave with a sinusoidal reference signal. The frequency of reference signal fixes the VSI output frequency and the DC voltage V_{dc} turns the fundamental amplitude and root mean square (RMS) output voltage.

The RMS of the VSI output voltage is expressed in (4)

$$V_{ac} = V_c \left[\sum_{m=1}^{2p} \frac{\delta_m}{\pi} \right]^{1/2} \quad (4)$$

Where p number of pulses and δ pulse width

2.4 Single Phase Induction Motor

The single phase induction motor is well suited for household appliances. It's have a modest performances compared to the three-phase asynchronous motor. The two windings of the SPIM and the capacitor C are often supplied from the mains. The SPIM may be represented by only two inductances, L_s and X , and two resistances, R_s and R_r . Equivalent dipoles, for forward and backward components, are those of Figure.4(a) and (b) [14].

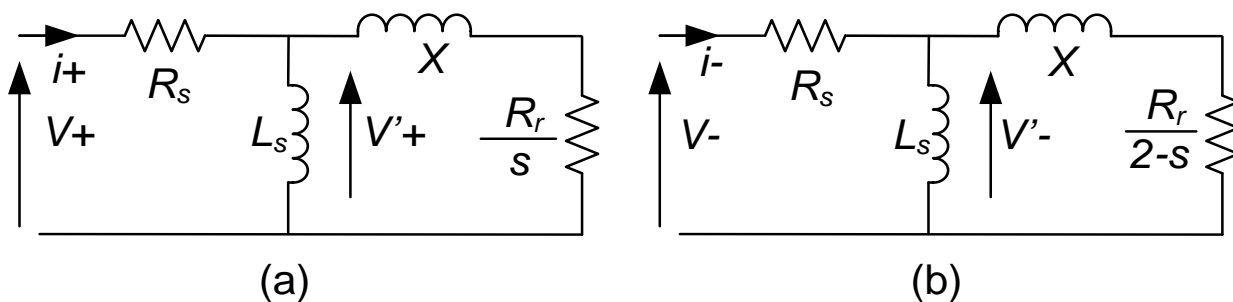


Figure.4. Equivalent dipoles for forward(a) and backward(b) components

Where R_s and L_s represent the stator windings resistance and inductance. The electromagnetic torque developed to drive the pump is done in (5)

$$T_{em} = p \cdot \frac{M}{L_r} (\Psi_{dr} i_{qs} - \Psi_{qr} i_{ds}) \quad (5)$$

The centrifugal pump acts as opposite load and its torque is done in (6):

$$T_{pu} = K_{pu} \Omega^2 \quad (6)$$

K_{pu} is a constant depending to the rated power of the pump.

3 Studied Multilevel Inverter Topologies

Two topologies have been studied in this work:

- Three level Inverter
- Five Level Inverter Topology.

3.1 Single Phase Three-Level Inverter Topology

The classical H-bridge inverter topology is depicted in figure.5-a. For bipolar PWM, the output waveform has three switching states. Its expression done (7) assumes to be odd quarter wave symmetry, whose amplitude (8) equals three levels $-V_{dc}, 0, +V_{dc}$.

$$V_{out}(\omega t) = \sum_{n=1,3,5,..}^{\infty} a_n \sin(n\omega t) \quad (7)$$

$$a_n = \frac{4V_{dc}}{n\pi} \sum_{k=1}^N (-1)^k \cos(n\alpha_k) \quad (8)$$

N is the number of switching angles per quarter-cycle.

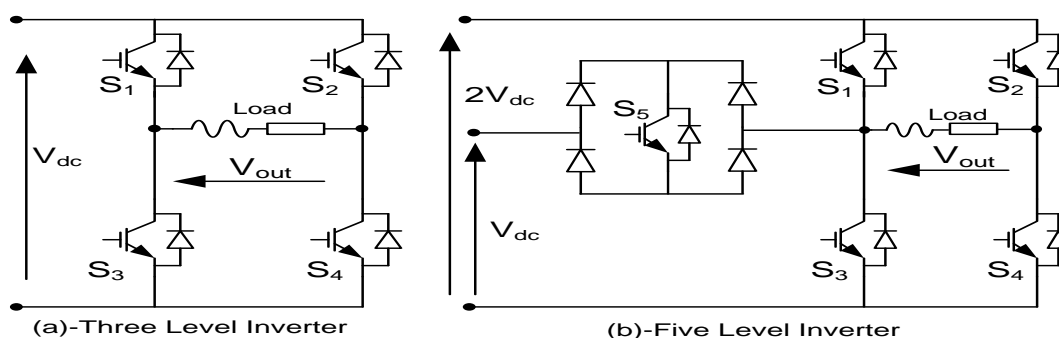


Figure.5. Three Level VSI (a) and Five Level VSI (b)

The transcendental equations characterizing the harmonic content can be converted into polynomial equations as in (8).

$$\begin{aligned} \frac{\pi V_1}{4V_{dc}} &= \cos(\alpha_1) - \cos(\alpha_2) + \cos(\alpha_3) - \cos(\alpha_4) + \cos(\alpha_5) \\ \frac{3\pi V_3}{4V_{dc}} &= \cos(3\alpha_1) - \cos(3\alpha_2) + \cos(3\alpha_3) - \cos(3\alpha_4) + \cos(3\alpha_5) \\ \frac{5\pi V_5}{4V_{dc}} &= \cos(5\alpha_1) - \cos(5\alpha_2) + \cos(5\alpha_3) - \cos(5\alpha_4) + \cos(5\alpha_5) \\ \frac{7\pi V_7}{4V_{dc}} &= \cos(7\alpha_1) - \cos(7\alpha_2) + \cos(7\alpha_3) - \cos(7\alpha_4) + \cos(7\alpha_5) \\ \frac{9\pi V_9}{4V_{dc}} &= \cos(9\alpha_1) - \cos(9\alpha_2) + \cos(9\alpha_3) - \cos(9\alpha_4) + \cos(9\alpha_5) \\ &\dots \end{aligned} \quad (9)$$

With V_1 Fundamental of the VSI output

Five unknowns, α_1 to α_5 , need to be solved in order to eliminate the 3rd, 5th, 7th, and 9th harmonics. For a desired amplitude of V_1 ; the nonlinear system describing harmonics contents will be set up as follows:

$$\begin{aligned}
 m &= \cos(\alpha_1) - \cos(\alpha_2) + \cos(\alpha_3) - \cos(\alpha_4) + \cos(\alpha_5) \\
 0 &= \cos(3\alpha_1) - \cos(3\alpha_2) + \cos(3\alpha_3) - \cos(3\alpha_4) + \cos(3\alpha_5) \\
 0 &= \cos(5\alpha_1) - \cos(5\alpha_2) + \cos(5\alpha_3) - \cos(5\alpha_4) + \cos(5\alpha_5) \\
 0 &= \cos(7\alpha_1) - \cos(7\alpha_2) + \cos(7\alpha_3) - \cos(7\alpha_4) + \cos(7\alpha_5) \\
 0 &= \cos(9\alpha_1) - \cos(9\alpha_2) + \cos(9\alpha_3) - \cos(9\alpha_4) + \cos(9\alpha_5)
 \end{aligned} \tag{10}$$

With $m = \frac{\pi V_1}{4V_{dc}}$

3.2 Single Phase Five-Level Inverter Topology

The single phase five-level voltage source inverter (FLVSI) topology is shown in the Figure.5-b. it's topology is based on a H-bridge inverter three states associated to a bidirectional switch with four diodes [11].

The VLSVSI has to generate five levels of voltage. i.e. $2V_{DC}, V_{DC}, 0, -V_{DC}, -2V_{DC}$. The half voltage level in the output voltage can be obtained by switching the auxiliary switch S5 properly. The VLSVSI output waveform is shown in Figure.6-b

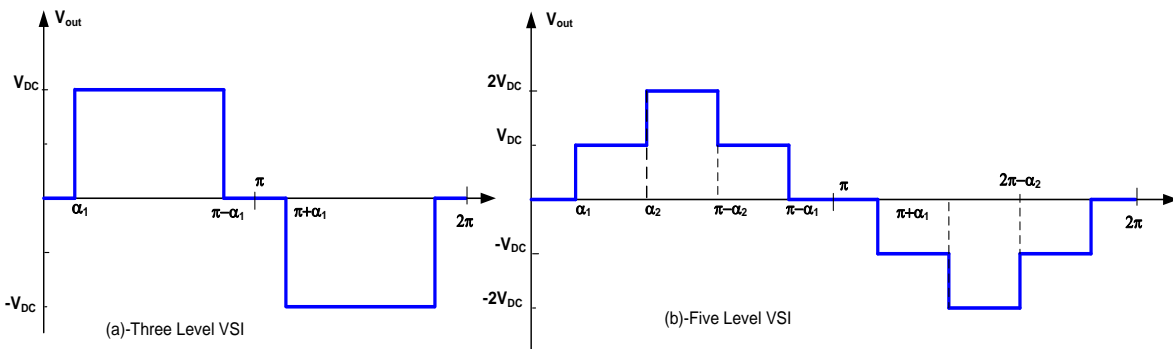


Figure.6. TLVSI and FLVSI voltage outputs waveform

The Fourier series expansion of V_{out} waveform output of the FLVSI is expressed in (11)

$$V_{out}(\omega t) = 4 \frac{V_{dc}}{n\pi} \sum_{n=1,3,5}^{\infty} [\cos(n\alpha_1) + \cos(n\alpha_2)]. \sin(n\omega t) \tag{11}$$

In order to eliminate the 3rd and 5th harmonics, only two angles are to solve from the nonlinear system describing harmonics as in (11):

$$\begin{aligned}
 m &= \cos(\alpha_1) + \cos(\alpha_2) \\
 0 &= \cos(3\alpha_1) + \cos(3\alpha_2) \\
 0 &= \cos(5\alpha_1) + \cos(5\alpha_2)
 \end{aligned} \tag{12}$$

With $m = \frac{\pi}{4} \cdot \frac{V_1}{2V_{dc}}$

The table I resume the switching pattern of all switches during one cycle for the two topologies. To solve switching angles, the Newton-Raphson method is applied, and a MATLAB program, is used to determine the optimized solutions of iterations. Two switching angles α_1 and α_2 , are to be calculated for the FLVSI.

Table 1. Switching patterns of the TLVSI and FLVSI

Three Level VSI					Five Level VSI					
S1	S2	S3	S4	Vout	S1	S2	S3	S4	S5	Vout
1	0	0	1	V_{DC}	0	0	0	1	1	V_{DC}
1	1	0	0	0	1	0	0	1	0	$2 V_{DC}$
0	0	1	1	0	0	0	1	1	0	0
0	1	1	0	$-V_{DC}$	1	1	0	0	0	0
					0	1	0	0	1	$-V_{DC}$
					0	1	1	0	0	$-2 V_{DC}$

4. Deployment

SHE PWM is an optimizing algorithm that gives a superior harmonic performance in high power applications with the minimum switching frequency [15]. However, the main drawback of this technique is the computational difficulties. To determine switching angles based on criterion of eliminating selected harmonics; a computational process is lunched invoking some mathematical methods to solve a group of nonlinear equations. The result, which is a set of gating angles, is stored in look-up tables for the gating controller. This embedded operation is easy to implement on a midrange microcontroller family with modest performances.

Figure.7 illustrates a synopsis of command implementation on a PIC16F876 microcontroller (©MICROCHIP) of the two structures TLVSI and FLVSI.

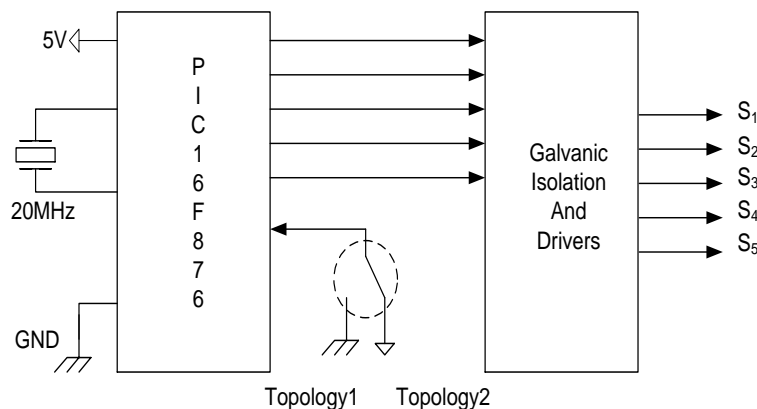


Figure.7. Topology Implementation

5. Simulation Results and Experimental Implementation

The PECS model has been simulated by using PSIM Copyright ©2001-2010 PowerSim Inc and considering an optimal irradiation. The PV panel are mounted in series delivering 60V to the two level boost chopper with a duty cycle $D=0.6$. The SPIM is modeled as an RL load.

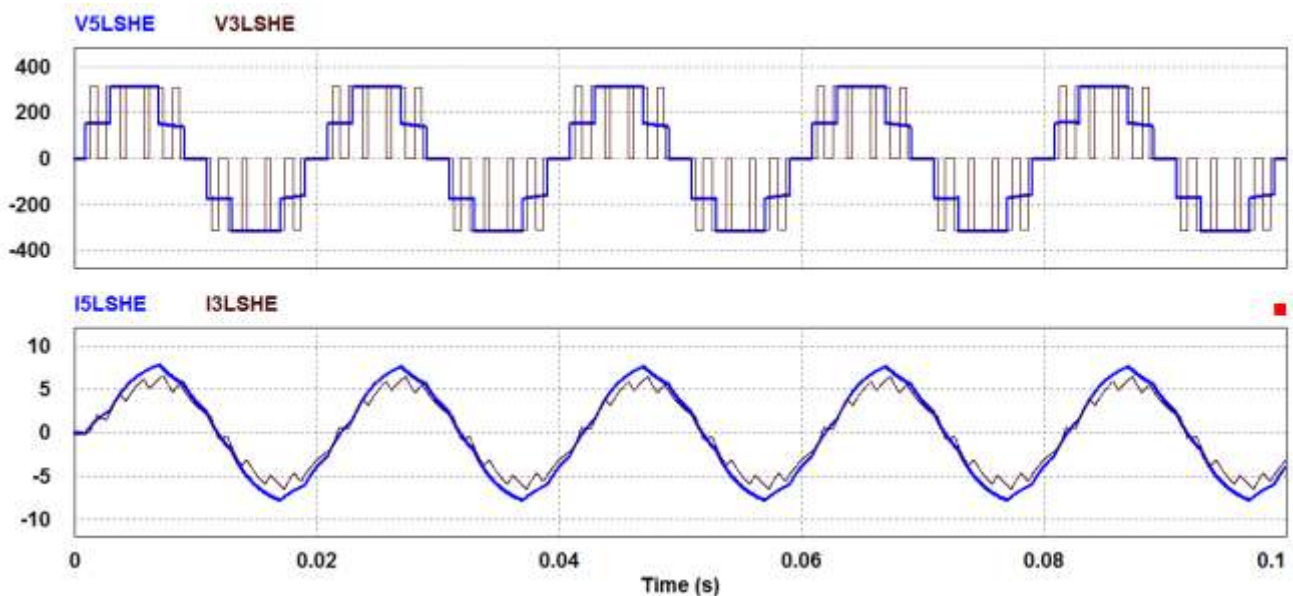


Figure.8. Current and Voltage output of the TLVSI and FLVSI

Figure.8 shows the waveforms of the currents and voltages of the output of the inverters. The voltage V5VSI (blue bold line) is the output of the five level version with three levels per half period. The Root Mean Square (RMS) value obtained is 223V and the Total Harmonic Distortion (THD) is just 19.2%.for the voltage V3VSI (black line), the RMS value is 220V and the THD reaches 75%. The currents are almost sinusoidal with a harmonic deformation for the TLVSI due to the number of switches commutations.

Figure.9 shows the voltages spectrum of the TLVSI and FLVSI. The SHE algorithm allows eliminating the 3rd, 5th,7th, and 9th harmonics for the TLVSI topology and reducing the 3rd and 5th harmonics for the FLVSI.

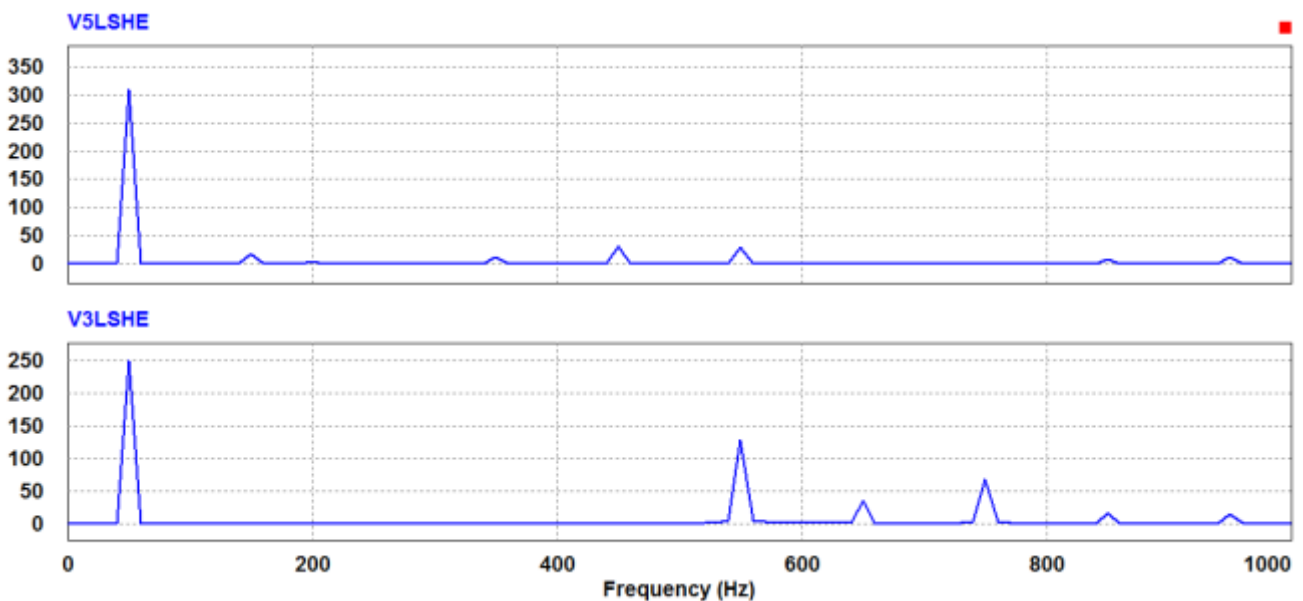


Figure.9. spectrum output voltage of the FLVSI and TLVSI

The two topologies of the VSI, were tested on a PECS platform mainly composed by a TLBC feeding the DC-AC inverter. The TLBC is used to output $2V_{DC}, V_{DC}$. The microcontroller card configures the inverter as 3 level H-bridge or 5level by generating the switching pattern according to the angle precalculated and stored in the flash memory. It's also activates the swithes to be used for each configuration. The modulation index was fixed to 0.85. Figure.10 and Figure.11 show the experimental results of both the current and voltage output and their spectrum for the FLVSI topology. For the TLVSI topology, the current and voltage output and their spectrum are depicted in Figure.12 and Figure.13.

From Figures 10 to 13, it can be seen, that the forms of voltage and current output are identical to the simulation results in Figure.8 and Figure.9. The frequency is 50Hz. The RMS value of the output voltage nears 220V. The spectrum responses of booth topologies depicted in figure.11 and Figure.13show that the order of the first harmonic appearing after the fundamental is 11 for the TLVSI and the 7 for the FLVSI.

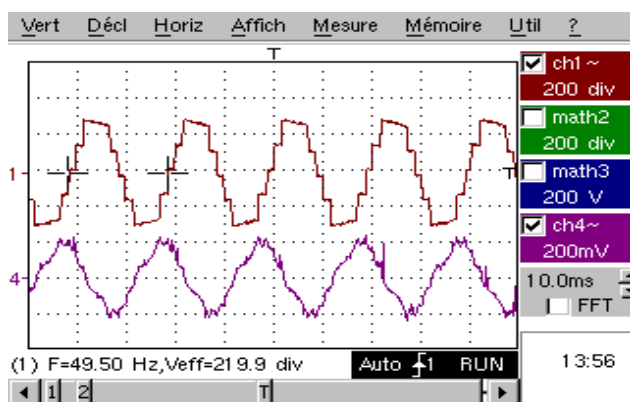


Figure.10. Voltage and Current Output of the FLVSI

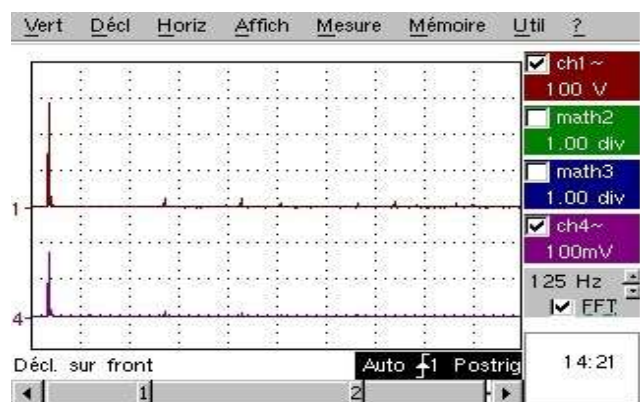


Figure.11. Voltage and Current Spectrum of the FLVSI

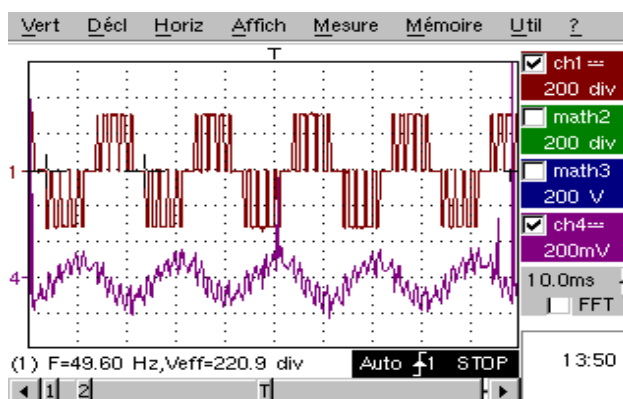


Figure.12. Voltage And Current Output of the TLVSI

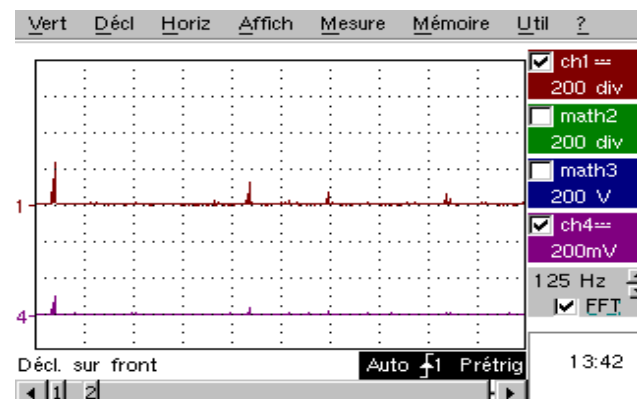


Figure.13. Voltage and Current Spectrum of the TLVSI

6. Conclusion

This paper has presented two structure of single phase inverter for PECS. The performance of both has been analyzed. The two topologies studied are able to feed correctly the SPIM with minimum number of switches. They offer improved output waveforms and permit to attain better efficiency. The THD and the switching losses in the five-level inverter is less than the other structure. However, the third-level inverter uses fewer switches and can be considered as an attractive solution for pumping combining both performance and cost.

References

- [1]. A. Hassoune, M. Khafallah, A. Mesbahi, and D. Breuil, "Electrical design of a photovoltaic-grid system for electric vehicles charging station," 14th International Conference on Systems, Signals & Devices (SSD 17) Marrakech, Morocco, 2017 pp. 228–233.
- [2]. A.Nouaiti, A.Saad, A.Mesbahi, M.Khafallah, M.Reddak "Single phase seven-level inverter for PV solar pumping system" International Renewable and Sustainable Energy Conference (IRSEC16) Marrakech, Morocco, 2016 pp. 474 – 478.
- [3]. I. D. Pharne and Y. N. Bhosale, "A review on multilevel inverter topology," in 2013 International Conference on Power, Energy and Control (ICPEC), 2013, pp. 700–703.
- [4]. R. P. Vishvakarma, S. P. Singh, and T. N. Shukla, "Multilevel inverters and its control strategies: A comprehensive review," in 2012 2nd International Conference on Power, Control and Embedded Systems (ICPCES), 2012, pp. 1–9.
- [5]. K. K. Gupta and S. Jain, "Comprehensive review of a recently proposed multilevel inverter," IET Power Electronics, vol. 7, no. 3, pp. 467–479, Mar. 2014.
- [6]. J. Rodriguez, Jih-Sheng Lai and Fang Zheng Peng, "Multilevel inverters: a survey of topologies, controls, and applications," in IEEE Transactions on Industrial Electronics, vol. 49, no. 4, pp. 724-738, Aug 2002.
- [7]. M. M. Renge and H. M. Suryawanshi, "Five-Level Diode Clamped Inverter to Eliminate Common Mode Voltage and Reduce in Medium Voltage Rating Induction Motor Drives," in IEEE Transactions on Power Electronics, vol. 23, no. 4, pp. 1598-1607, July 2008.
- [8]. R. Stala et al., "Results of Investigation of Multicell Converters With Balancing Circuit—Part I," in IEEE Transactions on Industrial Electronics, vol. 56, no. 7, pp. 2610-2619, July 2009.
- [9]. Jing Huang and K. A. Corzine, "Extended operation of flying capacitor multilevel inverters," in IEEE Transactions on Power Electronics, vol. 21, no. 1, pp. 140-147, Jan. 2006.
- [10]. F.Z.Peng, "A generalized multilevel inverter topology with self voltage balancing," in IEEE Transactions on Industry Applications, vol. 37, no. 2, pp. 611-618, Mar/Apr 2001.
- [11]. N. A.Rahim, K. Chaniago and J. Selvaraj, "Single-Phase Seven-Level Grid-Connected Inverter for Photovoltaic System," in IEEE Transactions on Industrial Electronics, vol. 58, no. 6, pp. 2435-2443, June 2011.
- [12]. A. Mesbahi, A. Saad, M. Khafallah O. Bouattane, and A. Raihani "Boost Converter analysis to optimise variable speed PMSG Wind Generation System" . 1st Annual Conference on Renewable and Sustainable Energy Conference IRSEC'2013, Ouarzazate, Morocco, 2013, pp 275-280.
- [13]. J. C. Rosas-Caro; J. M. Ramirez; P. M. Garcia-Vite, "Novel DC-DC Multilevel Boost Converter" Power Electronics Specialists Conference, 2008. Pages 2146 - 2151 .
- [14]. P. Vas, "Electrical machines and drives, a space vector theory approach", Ed. Oxford, 1992, pp 502-511
- [15]. J. N. Chiasson, L. M. Tolbert, K. J. McKenzie and Zhong Du, "A complete solution to the harmonic elimination problem," in IEEE Transactions on Power Electronics, vol. 19, no. 2, pp. 491-499, March 2004.